bioRxiv preprint doi: https://doi.org/10.1101/299248; this version posted April 11, 2018. The copyright holder for this preprint (which was not certified by peer review) is the author/funder, who has granted bioRxiv a license to display the preprint in perpetuity. It is made available under aCC-BY-NC-ND 4.0 International license.

1 # Mercury methylating microbial communities of boreal forest soils

2 Jingying Xu[1,*], Moritz Buck[1], Karin Eklöf[2], Omneya Osman[1], Jeffra K. Schaefer[3], Kevin Bishop[2], Erik
3 Björn[4], Ulf Skyllberg[5], Stefan Bertilsson[1], Andrea G. Bravo[1,6,*]

4 [1] *Department of Ecology and Genetics, Limnology, Uppsala University, SE-75236, Uppsala, Sweden*

5 [2] *Department of Aquatic Sciences and Assessment, Swedish University of Agricultural Sciences, SE-*
6 *75007, Uppsala, Sweden*

7 [3] *Department of Environmental Sciences, Rutgers University, New Brunswick, New Jersey 08901, USA*

8 [4] *Department of Chemistry, Umeå University, SE-901 87 Umeå, Sweden*

9 [5] *Department of Forest Ecology and Management, Swedish University of Agricultural Science, SE-901*
10 *83, Umeå, Sweden*

11 [6] *Department of Environmental Chemistry, Institute of Environmental Assessment and Water Research*
12 *(IDAEA), Spanish National Research Council (CSIC), C/Jordi Girona, 18-26 - E-08034 Barcelona –*
13 *Spain*

14

15 **Running tittle: Soil mercury methylating microbial communities**

16 *corresponding authors: jingying.xu@ebc.uu.se; jandriugarcia@gmail.com

17 **Abstract**

18 The formation of the potent neurotoxic methylmercury (MeHg) is a microbially mediated process that
19 has raised much concern because MeHg poses threats to wildlife and human health. Since boreal forest
20 soils can be a source of MeHg in aquatic networks, it is crucial to understand the biogeochemical
21 processes involved in the formation of this pollutant. High-throughput sequencing of 16S rRNA and the
22 mercury methyltransferase, *hgcA*, combined with geochemical characterisation of soils, were used to
23 determine the microbial populations contributing to MeHg formation in forest soils across Sweden. The
24 *hgcA* sequences obtained were distributed among diverse clades, including *Proteobacteria, Firmicutes*,
25 and *Methanomicrobia,* with *Deltaproteobacteria*, particularly *Geobacteraceae*, dominating the libraries
26 across all soils examined. Our results also suggest that MeHg formation is linked to the composition of
27 also non-mercury methylating bacterial communities, likely providing growth substrate (e.g. acetate) for
28 the *hgcA*-carrying microorganisms responsible for the actual methylation process. While previous

bioRxiv preprint doi: https://doi.org/10.1101/299248; this version posted April 11, 2018. The copyright holder for this preprint (which was not certified by peer review) is the author/funder, who has granted bioRxiv a license to display the preprint in perpetuity. It is made available under aCC-BY-NC-ND 4.0 International license.

29 research focused on mercury methylating microbial communities of wetlands, this study provides some
30 first insights into the diversity of mercury methylating microorganisms in boreal forest soils.
31
32 **Importance**
33 Despite a global state of awareness that mercury, and methylmercury in particular, is a neurotoxin that
34 millions of people continue to be exposed to, there are sizable gaps in our fundamental understanding of
35 the processes and organisms involved in methylmercury formation. In the present study we shed light on
36 the diversity of the microorganisms responsible for methylmercury formation in boreal forest soils. All
37 the microorganisms identified have a relevant role on the processing of organic matter in soils.
38 Moreover, our results show that the formation of methylation formation is not only linked to mercury
39 methylating microorganisms but also to the presence of non-mercury methylating bacterial communities
40 that contribute to methylmercury formation by the appropriate substrate to the microorganisms
41 responsible for the actual methylation process. This study improves current knowledge on the diversity
42 of organisms involved in methylmercury formation in soils.
43

44 INTRODUCTION

45 Mercury (Hg) is a potent toxin that might cause severe negative effects on wildlife and human health (1).
46 The toxicity of Hg is of such concern that 128 countries have signed the Minamata Convention, a global
47 treaty that entered into force in August 2017 with the explicit objective to reduce Hg emissions and
48 protect human health and the environment. High Hg emissions in the past have led to high present-day
49 Hg levels in different parts of the atmosphere, oceans and terrestrial ecosystems (2, 3). Because Hg has
50 a strong affinity for reduced sulphur or thiol (RSH) functional groups of soil organic matter (OM) (4, 5),
51 the increased atmospheric deposition of Hg during the industrialisation has resulted in high Hg
52 concentrations in organic-rich soils (6). As a consequence, the typically OM-rich soils in the boreal
53 biome has retained Hg deposition from both natural and anthropogenic emissions, and now represent an
54 important global Hg stock (4, 7).

bioRxiv preprint doi: https://doi.org/10.1101/299248; this version posted April 11, 2018. The copyright holder for this preprint (which was not certified by peer review) is the author/funder, who has granted bioRxiv a license to display the preprint in perpetuity. It is made available under aCC-BY-NC-ND 4.0 International license.

55 Soil OM has also been identified as a main vector of Hg and methylmercury (MeHg) transport from
56 catchments to surface waters in boreal areas (8, 9). Indeed, the mobilisation of inorganic Hg ($Hg^{(II)}$) and,
57 the more harmful, MeHg from soils by means of OM-mediated transport has been linked to MeHg
58 accumulation in lake sediments within catchments (9, 10) and in fish (11). As high MeHg levels in fish
59 have raised much concern in many boreal regions over the past decades (12, 13) and since forest soils
60 are an important site for MeHg formation (14), it is crucial to understand the processes and the
61 organisms involved in MeHg formation in boreal soils.

62 The methylation of $Hg^{(II)}$ to MeHg is biologically mediated (15) and takes place under oxygen deficient
63 conditions typical for wetlands (16), water logged soils (14), sediments (9) and anoxic water columns
64 (17), but can also occur in suspended particles in the aerobic zone of aquatic systems (18, 19). Specific
65 strains of sulphate-reducing bacteria (20, 21), iron reducing bacteria (FeRB) (22, 23), methanogens (24)
66 and Firmicutes (25) have the capability to methylate $Hg^{(II)}$. However, a number of factors controlling
67 bacterial activity and/or the geochemical speciation of inorganic $Hg^{(II)}$ will govern MeHg formation in
68 the environment (9, 26). For example, increases in temperature might lead to increases in biological
69 activity and accordingly also higher $Hg^{(II)}$ methylation rates (27). Redox potential also seems to be a key
70 factor as suboxic and mildly reducing conditions seem to promote high $Hg^{(II)}$ methylation rates,
71 whereas anoxic and strongly reducing conditions might lead to elevated sulphide concentrations that
72 eventually prevent $Hg^{(II)}$ from being available for methylation (28). Sulphur plays a major role in
73 influencing $Hg^{(II)}$ methylation by directly affecting the activity of some methylating bacteria (e.g.
74 sulphate reducing bacteria, SRB) and/or control the availability of $Hg^{(II)}$ for methylation (5). Specific
75 organic matter (OM) compounds can promote $Hg^{(II)}$ methylation by enhancing bacterial activity (9), but
76 also by defining $Hg^{(II)}$ speciation (29) and $Hg^{(II)}$ availability (30, 31). OM can also facilitate $Hg^{(II)}$
77 methylation by inhibiting mercury sulphide (HgS(s)) precipitation or enhance HgS(s) dissolution
78 thereby providing available $Hg^{(II)}$ for methylating microorganisms (32). High OM concentrations might
79 also decrease Hg methylation by formation of high mass molecular mass complexes that hamper $Hg^{(II)}$
80 availability (30). Recently it has been concluded that the availability of $Hg^{(II)}$ depends heavily on the $S^{(-II)}$
81 concentration in porewater and the RSH(aq)/RSH(ads) molar ratio of DOM (29). Together, all these

bioRxiv preprint doi: https://doi.org/10.1101/299248; this version posted April 11, 2018. The copyright holder for this preprint (which was not certified by peer review) is the author/funder, who has granted bioRxiv a license to display the preprint in perpetuity. It is made available under aCC-BY-NC-ND 4.0 International license.

82 studies highlight that geochemical conditions are key in determining the availability of $Hg^{(II)}$ and the
83 activity of the microbial communities involved in the process.

84 The identification of two functional genes, *hgcA* and *hgcB*, which play essential roles in $Hg^{(II)}$
85 methylation (15), provided the means to more directly characterise the complexity of microbial
86 communities involved in the formation of MeHg in natural ecosystems. This approach has been applied
87 to marshes, sediments and swamps in several geographic regions (33–36); rice paddies in China (37),
88 and water conservation areas of the northern Everglades, USA (38). However, very little work to date
89 has been conducted to reveal the distribution of microbial groups responsible for $Hg^{(II)}$ methylation in
90 forest soils within the vast boreal biome. To the best of our knowledge, no studies have directly
91 described the composition and spatial variation in $Hg^{(II)}$ methylating microbial communities in such
92 forests. Therefore, the primary goal of this paper was to describe $Hg^{(II)}$ methylating microbial
93 communities in various boreal forest soils and identify soil characteristics important for shaping these
94 communities. High-throughput next generation sequencing of amplified 16S rRNA and *hgcA* genes
95 combined with molecular barcoding and detailed soil geochemical characterisations were performed to
96 study the $Hg^{(II)}$ methylating microbial communities in 200 soil samples from three different boreal forest
97 regions in order to shed light on the biogeography of microorganisms responsible for MeHg formation
98 in the boreal landscape.

99 # RESULTS

100 ## Bacterial community composition in boreal forest soils

101 Soil samples were collected from 200 sites in October 2012 and were distributed across eight
102 catchments in three boreal forest regions in Sweden (Table S1, Table S2). A total of 3 321 197 high
103 quality 16S rRNA sequences remained after quality control and chimera removal (7–72 911 reads per
104 sample). The sample with only 7 reads was removed, and we then rarefied the rest of the data to the
105 remaining sample with the fewest reads (1692 reads). The final rarefied sequence dataset (329 940 reads)
106 clustered into 33 158 operational taxonomic units (OTUs) using a similarity threshold of 97 %. In the
107 rarefied dataset, 35 taxa at phyla level, 69 taxa at class level, 119 taxa at order level, and 187 taxa at

bioRxiv preprint doi: https://doi.org/10.1101/299248; this version posted April 11, 2018. The copyright holder for this preprint (which was not certified by peer review) is the author/funder, who has granted bioRxiv a license to display the preprint in perpetuity. It is made available under aCC-BY-NC-ND 4.0 International license.

108 family level were detected from all the soil samples across three regions. The overall coverage of the
109 forest bacterial community is reflected in the combined richness detected for random subsets of
110 analysed samples. The logarithmic shape indicated that most of the considerable OTU richness
111 occurring in the forest soils was accounted for in the combined dataset (Fig. S1). Among the dominant
112 phyla across all regions (>5 % relative abundance), *Acidobacteria* was the most abundant, followed by
113 *Proteobacteria, Planctomycetes, Bacteroidetes, Parcubacteria and Verrucomicrobia* (Table 1).
114 Combined, these phyla accounted for 77.5 % of the total sequences (Table 1). Most of the previously
115 identified clades known to contain $Hg^{(II)}$ methylators (25, 39) were detected in the present study,
116 including *Deltaproteobacteria* (3.31 % of the total reads), *Chloroflexi* (2.60 % of the total reads),
117 *Firmicutes* (0.77 % of the total reads) and *Euryarchaeota* (0.66 % of the total reads) (Table 1).
118 Microbial community composition based on 16S rRNA sequences in the 34 studied MeHg hotspots
119 showed a similar pattern in terms of the dominant phyla (>5 % relative abundance), with *Acidobacteria*
120 and *Proteobacteria* being the most abundant ones. However, *Bacteroidetes* and *Chloroflexi* contributed
121 much more to the total communities at these hotspots compared to the combined dataset across all 200
122 samples (Table 1).

123 A non-metric multidimensional scaling (nMDS) plot based on 16S sequences was used to visualise the
124 composition of the bacterial community among samples. *Unclassified Acidobacteriales, Unclassified*
125 *Ignavibacteriales, Spirochaetaceae, Holophagaceae*, *Anaerolineaceae, Betaproteobacteria and*
126 *Tepisiphaeraceae* were important contributing families for shaping the differences in bacterial
127 community composition among samples (Fig. 1). Geochemical factors that were correlated (correlation
128 coefficients > 0.5) with the bacterial composition were projected on top with longer vectors implying
129 stronger correlations (Fig. 1). %MeHg, reflected by bubble sizes, presented a strong coupling to the
130 bacterial community composition, which was further confirmed by %MeHg presenting a long vector
131 among all the geochemical factors (Fig. 1). Water content, C%, S% and N% were all found to be the
132 factors that affected the composition of soil bacterial community (Fig. 1), indicating that a supply of
133 organic matter and nutrients in the moist soil shapes the bacterial community. This is in agreement with
134 previous research that pointed out the contribution of nutrients and organic matter to bacterial activities

bioRxiv preprint doi: https://doi.org/10.1101/299248; this version posted April 11, 2018. The copyright holder for this preprint (which was not certified by peer review) is the author/funder, who has granted bioRxiv a license to display the preprint in perpetuity. It is made available under aCC-BY-NC-ND 4.0 International license.

135 and $Hg^{(II)}$ methylation (9, 28). Also, S was well correlated with both C and N (Table S3), suggesting that
136 most of the measured sulphur in the sampled soils has likely an organic origin. This has been found as a
137 common feature in boreal soils (40–42).

138 *Unclassified Fibrobacterales, Methanosaetaceae, Unclassified Ignavibacteriales, Spirochaetaceae,*
139 *Holophagaceae* and *Anaerolineaceae* exhibited the highest correlations with %MeHg (Table 2).
140 *Syntrophobacteraceae, Methanosarcinaceae, Methanoregulaceae, Desulfobulbaceae, Syntrophaceae,*
141 *Desulfobacteraceae* and *Dehalococcoidaceae*, which potentially host $Hg^{(II)}$ methylators (25, 39), were
142 also found relevant to the bacterial community composition in high-%MeHg sites (Table 2).

143 **Figure 1.**

144 Distribution of $Hg^{(II)}$ methylators

145 The samples with high soil MeHg concentrations and %MeHg > 1% were defined as "MeHg hotspots".
146 In 34 MeHg hotspots (see soils geochemistry descriptors in Table S4, n = 34), the relative abundance of
147 microbial families carrying representatives known to methylate $Hg^{(II)}$ was assessed based on *hgcA*
148 sequences (25, 39). A total of 1 257 577 *hgcA* sequences remained after quality control and chimera
149 removal (11 404–55 461 reads per sample). The *hgcA* dataset was rarefied to the remaining sample with
150 the fewest reads (11 404 reads). The rarefied sequence dataset accounted a total of 387 736 reads that
151 clustered into 573 operational taxonomic units (OTUs) using a similarity threshold of 97 %. As for the
152 16 rRNA, the logarithmic shape indicated that most of the considerable species richness of $Hg^{(II)}$
153 methylators occurring in the forest soils was accounted for in the combined dataset (Fig. S1).
154 Representative sequences from 22 families were found in the 34 analysed MeHg hotspots. Of all the
155 *hgcA* sequences, 3.13 % were not taxonomically assigned (Unclassified), 0.28 % were unclassified
156 *Euryarchaeota*, and 7.28 % could not be assigned beyond the rank of Bacteria (Unclassified Bacteria).

157 The majority of the sequences annotated to the level of family clustered with *Deltaproteobacteria*,
158 making up 85.4 % of all the *hgcA* reads (Table 3). The remaining classified *hgcA* sequences were
159 distributed across diverse families affiliated to *Firmicutes* and *Methanomicrobia*. *Unclassified*
160 *Deltaproteobacteria* represented up to 56 % of the reads and among the identified families,

bioRxiv preprint doi: https://doi.org/10.1101/299248; this version posted April 11, 2018. The copyright holder for this preprint (which was not certified by peer review) is the author/funder, who has granted bioRxiv a license to display the preprint in perpetuity. It is made available under aCC-BY-NC-ND 4.0 International license.

161 *Geobacteraceae* were the most abundant, contributing up to 40 % in Strömsjöliden. *Ruminococcaceae*
162 (3.21 % of all *hgcA* reads) occurred as another important family in the hotspots in Örebro; while
163 methanogens and syntrophic lineages were less abundant in the hotspots based on *hgcA* sequences
164 (Table 3).

165 *Unclassified Desulfuromonadales, Geobacteraceae, Ruminococcaceae, unclassified Desulfovibrionales,*
166 *Desulfovibrionaceae, and unclassified Deltaproteobacteria* seemed to contribute to differences in the
167 composition of $Hg^{(II)}$ methylators in the studied soils (Fig. 2a). Among the measured geochemical
168 parameters, the S% and the C/S seemed to have an impact on shaping the community composition of
169 $Hg^{(II)}$ methylators (Fig. 2b). Moreover, *Methanoregulaceae, Desulfovibrionaceae,*
170 *Desulfuromonadaceae, Desulfarculaceae* and *Methanomassiliicoccaceae* correlated positively with S%
171 and negatively with C/S (Table S5). In the studied MeHg hotspots, S was strongly correlated with both
172 C and N (Table S6), suggesting most of the measured sulphur in the hotspots is also likely presented in
173 organic forms.

174

175 Phylogenetic analysis of *hgcA* genes

176 All the *Proteobacteria* families belonged to *Deltaproteobacteria*, a class with which most currently
177 confirmed $Hg^{(II)}$-methylating bacteria are affiliated (43, 44). When combined, the 20 most abundant
178 OTUs accounted for 72 % of the total reads. Noteworthy, phylogenetic analysis revealed that the most
179 abundant $Hg^{(II)}$-methylating OTUs ("OTU_0005", "OTU_0705", "OTU_0008", and "OTU_0012") in
180 the studied forest soils were either taxonomically assigned as *Geobacter sp. or* phylogenetically related
181 to *Geobacter* species (Fig. 3). Among the 20 most abundant OTUs, 17 were taxonomically annotated as
182 *Deltaproteobacteria.* Among these 17 OTUs, 9 were taxonomically annotated as *Geobacter* and 8 were
183 phylogenetically related to *Geobacter* species (Fig. 3). Summing the identified *Geobacter* and the OTUs
184 phylogenetically related to *Geobacter* species, these 17 OTUs accounted for 62 % of the total *hgcA*
185 reads. The 5th most abundant OTU and was taxonomically denoted as *Firmicutes* (*Ethanoligenens*) and
186 the 6th and 7th could not be annotated beyond the bacterial domain.

187

bioRxiv preprint doi: https://doi.org/10.1101/299248; this version posted April 11, 2018. The copyright holder for this preprint (which was not certified by peer review) is the author/funder, who has granted bioRxiv a license to display the preprint in perpetuity. It is made available under aCC-BY-NC-ND 4.0 International license.

188 # DISCUSSION

189 ## Community composition of $Hg^{(II)}$ methylators in boreal forest soils

190 Among the diverse microbial communities seen in the soil samples (Table 1), most of the previously
191 identified $Hg^{(II)}$ methylating groups, e.g., *Deltaproteobacteria, Chloroflexi, Firmicutes and*
192 *Euryarchaeota* could be detected (Table 3). *Deltaproteobacteria* have been considered a predominant
193 $Hg^{(II)}$ methylating class in anaerobic soils (34, 37, 38). In the present study, *Deltaproteobacteria* were
194 also the predominant $Hg^{(II)}$ methylators at the hotspots with *Geobacteraceae* as the most represented
195 family. This family alone contributed over 30% of all *hgcA* reads, and their importance could be seen at
196 all the sampled sites and particularly in Strömsjöliden (Table 3). Iron reducing bacteria (FeRB) have
197 previously been shown to be important for $Hg^{(II)}$ methylation in some environments (22, 23, 36, 43), and
198 most *Geobacter* tested so far are particularly efficient at MeHg formation in the laboratory (23). This
199 suggests that the ability to methylate $Hg^{(II)}$ is widely distributed and a typical feature among the
200 *Geobacteraceae*. The lack of a specific inhibitor for FeRB have hindered the quantification of the
201 relative contribution of FeRB compared to SRB (i.e molybdate inhibitor) and methanogens (i.e.
202 Bromoethanesulfonate inhibitor) to MeHg formation. The discovery of the *hgcA* pushed the state of the
203 art and made possible to identify $Hg^{(II)}$ methylators in environment (15, 25). Our results combined with
204 previous findings in wetlands and paddy soils (34, 37, 38) highlight the importance of *Geobacteraceae*
205 as $Hg^{(II)}$ methylators in boreal forest soils and evidence their potentially very important roles in a wide
206 range of environments.

207 While SRB are considered to be the principal $Hg^{(II)}$ methylators in aquatic systems (27, 45–48), not
208 much information is available on $Hg^{(II)}$ methylators in soils. However, identified SRB in the hotspots
209 only accounted for a minor portion of $Hg^{(II)}$ methylators (Table 3). However, it is nevertheless plausible
210 that at least some of the *hgcA* sequences annotated as unclassified *Deltaproteobacteria* (Table 3) could
211 be unknown $Hg^{(II)}$ methylating SRB or even $Hg^{(II)}$ methylating sulphate-reducing syntrophs, capable of
212 syntrophic fermentation of simple organic acids in the absence of sulphate as the terminal electron
213 acceptor (49, 50). Therefore, we cannot discard the possibility that also SRB contribute significantly to
214 $Hg^{(II)}$ methylation in the studied systems. A previous study based on selective inhibitors and rate

bioRxiv preprint doi: https://doi.org/10.1101/299248; this version posted April 11, 2018. The copyright holder for this preprint (which was not certified by peer review) is the author/funder, who has granted bioRxiv a license to display the preprint in perpetuity. It is made available under aCC-BY-NC-ND 4.0 International license.

215 measurements indeed suggested SRB played an important role in MeHg formation in boreal forest soils
216 (41). Additionally it has been demonstrated that even when SRB belong to the 'rare biosphere' of
217 peatlands, they contribute significantly to respiration processes (51).

218 *Ruminococcaceae* belongs to another newly confirmed representative of $Hg^{(II)}$ methylators, the
219 *Firmicutes* (25). *Firmicutes* contributed to $Hg^{(II)}$ methylating microbial communities at the water
220 conservation areas of the Florida Everglades (38) but were not detected in boreal wetlands (34). In the
221 present study, *Ruminococcaceae* were prominent contributors to the *hgcA* pool in hotspots from Örebro
222 and in all soils from Strömsjöliden (Table 3). They could thus play a role in shaping the composition of
223 $Hg^{(II)}$ methylating community as further indicated by the negative correlation though weak between
224 *Ruminococcaceae* and C/S, a primary geochemical factor shaping $Hg^{(II)}$ methylating communities in the
225 hotspots (Table S5 and Fig. 2b). Not much research has been devoted to the possible relationship
226 between organic S and $Hg^{(II)}$ methylating *Ruminococcaceae*. Considering the abundance of this group in
227 forest soils, further efforts are needed to shed light on the metabolic or physiological pathways of $Hg^{(II)}$
228 methylating *Ruminococcaceae*.

229 Methanogens were early on suspected to be responsible for $Hg^{(II)}$ methylation (52), but not until recently
230 were they verified as a significant source of $Hg^{(II)}$ methylators in various environments (24, 34). In the
231 hotspots in the studied soils, they were also detected, though not very abundant in the $Hg^{(II)}$ methylating
232 microbial community. *Chloroflexi* has recently been identified as potential $Hg^{(II)}$ methylators in the
233 water conservation areas, paddy soils and wetlands (34, 38, 53). The *hgcA* data did not confirm any
234 significant role of this group in MeHg production in boreal forest soils (Table 3), even though 16S
235 rRNA data revealed non-$Hg^{(II)}$ methylating *Chloroflexi* (e.g. the class *Anaerolineae*) in soils from all
236 three regions (Table 1).

237 Previous studies have mainly explored flooded environments such as paddy soils (37), boreal wetlands
238 (34) and the water areas of the Florida Everglades (38). Hence our study provided important new
239 information on the composition and diversity of $Hg^{(II)}$ methylating microbial communities in non
240 flooded boreal forest soils and the boreal landscape, and in doing so identified *Geobacteraceae* as
241 significant $Hg^{(II)}$ methylators in the terrestrial biome. The diversity of $Hg^{(II)}$ methylators described in

bioRxiv preprint doi: https://doi.org/10.1101/299248; this version posted April 11, 2018. The copyright holder for this preprint (which was not certified by peer review) is the author/funder, who has granted bioRxiv a license to display the preprint in perpetuity. It is made available under aCC-BY-NC-ND 4.0 International license.

242 this study need to be interpreted cautiously. The *hgcA* gene was only recently discovered and the
243 optimization of the appropriate methods and, in particular the design of primers for the *hgcA*
244 amplification, is still developing (54). Additionally, DNA based methods only reveal the presence of
245 organisms, while alternative approaches based on transcription data, proteomes or rate measurements
246 are needed for verifying their activity. Our data nevertheless provide new insights about $Hg^{(II)}$
247 methylating microbial communities in boreal forest soils and can as such guide and serve as a resource
248 for future research efforts in this field.

249 Bacterial communities fuel $Hg^{(II)}$ methylators

250 %MeHg has previously been used as a proxy for methylation efficiency (55, 56), and high %MeHg has
251 also in a few cases been shown to correlate positively with the abundance of $Hg^{(II)}$ methylators (14, 57).
252 In the current study, sites with high %MeHg featured bacterial communities different from those
253 observed at sites with low % MeHg (Fig. 1). Although, families known to contain $Hg^{(II)}$ methylators
254 (*Syntrophobacteraceae, Methanosarcinaceae, Methanoregulaceae, Desulfobulbaceae, Syntrophaceae,*
255 *Desulfobacteraceae* and *Dehalococcoidaceae*; 25) were found at sites with high %MeHg, there were
256 also positive correlations between %MeHg and families that are not known to host $Hg^{(II)}$ methylators,
257 such us *Unclassified Fibrobacterales, Methanothrix* (formerly *Methanosaeta*), *Unclassified*
258 *Ignavibacteriales, Spirochaetaceae, Holophagaceae* and *Anaerolineaceae* (Table 2). This suggests that
259 not only the $Hg^{(II)}$ methylators themselves, but also the supporting and interacting bacterial communities
260 residing in the soil environment may influence MeHg formation across the studied regions.
261 *Anaerolineaceae, Spirochaetaceae* and *Holophagaceae* are for example known to generate acetate by
262 fermentation processes (58). *Fibrobacterales*, have recently been suggested to have an important role in
263 cellulose hydrolysis in anaerobic environments, including soils (59). The *Ignavibacteria* class was
264 recently described (Iino et al., 2010) and the physiology and metabolic capacities of this group is still
265 poorly known, even if a distinctive feature of this group is the ability to grow on cellulose and its
266 derivatives with the utilization of Fe(III) oxide as electron acceptor (60). It may well be that these
267 families, which correlated well with %MeHg (Table 2) and seem to be involved in the degradation of
268 long chain OM compounds (61, 62), promoted MeHg production by providing appropriate substrates

bioRxiv preprint doi: https://doi.org/10.1101/299248; this version posted April 11, 2018. The copyright holder for this preprint (which was not certified by peer review) is the author/funder, who has granted bioRxiv a license to display the preprint in perpetuity. It is made available under aCC-BY-NC-ND 4.0 International license.

269 (e.g. acetate) for the $Hg^{(II)}$ methylators. $Hg^{(II)}$ methylators and non-$Hg^{(II)}$ methylating members of
270 *Desulfobulbaceae*, known to oxidise organic substrates incompletely to acetate (63), might also have
271 provided the necessary substrate to $Hg^{(II)}$ methylators (Table 2). Based on our results, we propose an
272 important role of also the non-$Hg^{(II)}$ methylating bacterial heterotrophs in sustaining the activity of the
273 $Hg^{(II)}$ methylating microorganisms and thereby influencing MeHg formation in boreal forest soils.
274 Moreover, the correlation between *Methanothrix* and %MeHg deserves special attention. It has been
275 shown that *Methanothrix* can establish syntrophic cooperation with *Anaerolineaceae* (61) or
276 *Geobacteraceae* (64) in methanogenic degradation of long chain carbon compounds (alkanes). As our
277 results show that *Geobacteraceae* are major contributors to the $Hg^{(II)}$ methylating microbial community
278 (Table 3), the high correlation found between *Methanothrix* and %MeHg could be the result of the
279 interaction between the non-$Hg^{(II)}$ methylating *Methanothrix* and the $Hg^{(II)}$ methylating *Geobacteraceae.*
280 In brief, we provide novel system-level information on putative trophic interactions between non-$Hg^{(II)}$
281 methylating and the $Hg^{(II)}$ methylating taxa. We further suggest that more in depth studies with
282 metagenome-level sequencing and metabolic pathway reconstruction will be a logical next step to gain a
283 more complete understanding of how $Hg^{(II)}$ methylating bacterial and archaeal species interact in soils.

284 ## CONCLUSIONS

285 A newly developed strategy that combine high-throughput *hgcA* amplicon sequencing with molecular
286 barcoding revealed diverse clades of $Hg^{(II)}$ methylators in forest soils. This study confirms a
287 predominant role of *Deltaproteobacteria*, and in particular *Geobacteraceae,* as key $Hg^{(II)}$ methylators in
288 boreal forest soils. *Firmicutes*, and in particular *Ruminococcaceae*, were also abundant members of the
289 $Hg^{(II)}$ methylating microbial community. Besides the identified $Hg^{(II)}$ methylators, we suggest that the
290 non-$Hg^{(II)}$-methylating bacterial community (e.g. *Anaerolineaceae, Holophagaceae* and
291 *Spirochaetaceae*) might have contributed to the net MeHg formation (%MeHg) by processing OM and
292 thereby providing low OM compounds as a substrate to $Hg^{(II)}$ methylators (e.g acetate). By revealing
293 linkages between $Hg^{(II)}$ methylators and non- $Hg^{(II)}$ methylators, our results calls for further community-
294 level work on the metabolic interactions in soil microbial communities to understand $Hg^{(II)}$ methylation.

bioRxiv preprint doi: https://doi.org/10.1101/299248; this version posted April 11, 2018. The copyright holder for this preprint (which was not certified by peer review) is the author/funder, who has granted bioRxiv a license to display the preprint in perpetuity. It is made available under aCC-BY-NC-ND 4.0 International license.

295 Such studies would need to go beyond the $Hg^{(II)}$ methylating microbial populations. Our findings
296 provide a better understanding of $Hg^{(II)}$ methylating microbial communities in forest soils and the boreal
297 landscape.

298 ## MATERIALS AND METHODS

299 ### Site description

300 Soil samples were collected from 200 sites in October 2012 and were distributed across eight
301 catchments in three boreal forest regions in Sweden (Table S1 and S2). Within each of the catchments,
302 25 samples were collected. The most southern region Örebro (59°10′16.39″N 14°34′3.01″E) includes
303 three catchments and the sampled soils are dominantly Podzol with Histosols (65) in the lower parts of
304 the catchments along the streams. The organic matter (O) horizons were most often thicker than 20 cm.
305 More detailed information is given in Eklöf et al. (66). Two northern regions, Balsjö (64°1′37″N
306 18°55′43″E) and Strömsjöliden (64°6′48″N 19°7′36″E), are located 600–700 km north of Örebro and
307 around 14 km apart from each other. Balsjö includes three catchments dominated by orthic Podzol, with
308 Histosols along the streams. The O horizons were most often thicker than 10–20 cm in the lower parts
309 and less than 10 cm higher up in the catchments. More details are given in Löfgren *et al*. (2009).
310 Strömsjöliden includes two catchments and the soils are dominated by fine-grained moraine. The
311 organic layers are most often less than a few centimetres deep. The samples with high soil MeHg
312 concentrations and %MeHg > 1% were defined as "MeHg hotspots" (n=34), see a summary of the soil
313 characteristics of "MeHg hotspots" in Table S4.

314 The daily mean air temperatures during the 9 sampling days in September in 2012 varied between 7 and
315 12 °C in Örebro catchments and 4 and 11 °C in Balsjö and Strömsjöliden catchments. There were no
316 major rain events during the sampling period and the temperature and precipitation was normal for the
317 time of the year.

318 ### Soil sampling

319 Soil samples were collected with a soil coring tube (Ø=23 mm). In each catchment, around half of the
320 samples (n=12) were collected systematically along the topographic fall line of the hill slope, at set

bioRxiv preprint doi: https://doi.org/10.1101/299248; this version posted April 11, 2018. The copyright holder for this preprint (which was not certified by peer review) is the author/funder, who has granted bioRxiv a license to display the preprint in perpetuity. It is made available under aCC-BY-NC-ND 4.0 International license.

321 distances from the stream draining the area. These samples were collected from the upper 6 cm of the O
322 horizons or the whole O horizons if these were less than 6 cm deep. The locations of the remaining
323 sampling sites (n=13) were chosen by actively looking for potential hot spots for MeHg formation, such
324 as wet patches, driving tracks and stump holes. These targeted samples were also collected from various
325 depths, e.g. depths where groundwater levels were most frequently fluctuating were of special interest
326 for potential $Hg^{(II)}$ methylation.

327 Single-use plastic gloves were used and soil samples for chemical analyses were collected in plastic
328 bags or acid washed Falcon tubes and stored on ice in a cooler during transport to the laboratory (within
329 8 hours). Soil samples for molecular analyses were collected following adequate aseptic sampling
330 protocols. All sampling equipment was sterilized by washing in 70% ethanol in between samples.
331 Samples were collected in sterilized plastic tubes and frozen in liquid nitrogen directly in the field, and
332 then stored at -80°C until further processing and analyses.

333 Chemical analyses

334 Soil samples were analysed for total Hg (THg), MeHg, water content, and mass percentage of carbon
335 (C), nitrogen (N) and sulphur (S). Samples were freeze-dried and ground by hand in a mortar prior to
336 analyses for THg, C%, N% and S%. Wet and dry weights were measured to estimate the water content.
337 Total Hg was measured using a Perkin Elmer SMS100 total Hg analyser in accordance with US EPA
338 method 7473. The method includes a thermal decomposition step, followed by amalgamation and
339 atomic absorption spectrophotometric detection (working range 0.05–600 ng). Reproducibility and
340 accuracy of measurements were checked by analyses of replicate samples and reference standards.
341 Analyses of MeHg were done by using GC-ICPMS (68) on fresh samples immediately after thawing. C,
342 N and S were analysed on dry soils packed tightly in tin capsules (Elemental Microanalysis, 6.4 mm)
343 and subsequently measured by high temperature catalytic oxidation with a COTECH ECS 4010
344 elemental analyser calibrated with sulfanilamide standard (C 41.84 %, N 16.27 %, H 4.68 %, O 18.58
345 %, S 18.62 %). Analytical precision was $< \pm 0.3$ % for C, ± 1.5 % for N and ± 3.5 % for S.

346 Microbiological analyses

bioRxiv preprint doi: https://doi.org/10.1101/299248; this version posted April 11, 2018. The copyright holder for this preprint (which was not certified by peer review) is the author/funder, who has granted bioRxiv a license to display the preprint in perpetuity. It is made available under aCC-BY-NC-ND 4.0 International license.

347 **16S rRNA gene:** Microbial DNA was extracted from soil samples using the Power soil DNA
348 isolation Kit (MoBio Laboratories Inc, CA, USA) and the quality of the extracted DNA was assessed by
349 gel electrophoresis (1% agarose). Bacterial 16S rRNA genes were amplified in two steps polymerase
350 chain reaction (PCR) according to the protocol in Sinclair *et al* (2015). Briefly, non-barcoded primers
351 Bakt_341F and Bakt_805R (Table S7) were used for the 1st PCR step of 20 cycles. The resulting PCR
352 products were diluted 100 times before being used as template in a 2nd PCR step of 10 cycles with
353 similar primers carrying sample-specific 7-base DNA barcodes. All PCRs were conducted in 20 µL
354 volume using 1.0 U Q5 high fidelity DNA polymerase (NEB, UK), 0.25 µM primers, 0.2 mM dNTP
355 mix, and 0.4 µg bovine serum albumin. The thermal program consisted of an initial 95 °C denaturation
356 step for 5 min, a cycling program of 95 °C for 40 seconds, 53 °C for 40 seconds, 72 °C for 60 seconds
357 and a final elongation step at 72 °C for 7 minutes. Amplicons from the 2nd PCR were purified using the
358 Qiagen gel purification kit (Qiagen, Germany) and quantified using a fluorescence-based DNA
359 quantitation kit (PicoGreen, Invitrogen). The final amplicons after two PCR steps were pooled in equal
360 proportions to obtain a similar number of sequencing reads per sample. Amplicon sequencing was
361 carried out following the protocol described in Sinclair *et al* (2015) using the MiSeq instrument.
362 Illumina sequencing was performed by the SNP/SEQ SciLifeLab facility hosted by Uppsala University
363 using 300bp chemistry. Chimera identification and OTU (Operational Taxonomic Unit) clustering by
364 denoising was done using UNOISE (from USEARCH version 9, ref. 70, 71). SINTAX (from
365 USEARCH version 9, ref. (72)) with the SILVA reference database (release 128) was used as a base to
366 taxonomically annotate OTUs. The sequence data has been deposited to the EBI Archive under
367 accession number PRJEB20882.

368 ***HgcA* gene:** Among the 50 samples selected based on having %MeHg >1 %, 34 resulted in positive
369 PCR amplification of the *hgcA* gene. The protein-coding gene *hgcA* which plays an essential role in Hg
370 methylation was amplified with previously published *hgcA* primers (*hgcA_ 261F* and *hgcA_912R*)
371 (Table S7, 34) modified for parallelized high-throughput Illumina sequencing. HPLC-purified primers
372 carrying Illumina adaptors at the 5' end (*hgcA_261F_Adaptor* and *hgcA_912R_Adaptor*, Table S7) were
373 here used for the 1st stage PCR. In the 2nd stage PCR, standard Illumina handles and barcode primers

bioRxiv preprint doi: https://doi.org/10.1101/299248; this version posted April 11, 2018. The copyright holder for this preprint (which was not certified by peer review) is the author/funder, who has granted bioRxiv a license to display the preprint in perpetuity. It is made available under aCC-BY-NC-ND 4.0 International license.

374 (Table S7) were used to enable pooling of all the samples for parallelized Illumina sequencing. *HgcA*
375 was first amplified in 50 μL volume with 1x Phusion GC Buffer, 0.2 mM dNTP mix, 5% DMSO, 0.1
376 μM of each adaptor-linked primer, 7 μg/μL BSA, 4 μL extracted DNA template, and 1.0 U Phusion high
377 fidelity DNA polymerase (NEB, UK) for an initial denaturation of 2 min at 98 °C followed by 35 cycles
378 (10 s at 96 °C, 30 s 56.5 °C and 45 s at 72 °C), and a final extension at 72°C for 7 min. Following this
379 initial step, a 2nd PCR was conducted to add sample-specific molecular barcodes. Reactions were carried
380 out in 20 μL volumes using 1x Q5 reaction buffer, 0.2 mM dNTP mix, 0.1 μM barcode primers, purified
381 1st PCR products and 1.0 U Q5 high fidelity DNA polymerase (NEB, UK) for an initial denaturation of
382 30 s at 98 °C followed by 18 cycles (10 s at 98 °C, 30 s 66 °C and 30 s at 72 °C), and a final extension
383 at 72°C for 2 min. The quality and size of the *hgcA* amplicons were assessed by gel electrophoresis and
384 GelRed visualization on a 1% agarose gel (Invitrogen, USA) prior to purification by Agencourt AMPure
385 XP (Beckman Coulter, USA) after both PCR steps. Quantifications of purified amplicons from the 2nd
386 stag PCR were performed using the PicoGreen kit (Invitrogen).

387 Amplicons were sequenced using the same method as for the 16S rRNA gene. Forward read
388 sequences were only used in data analysis due to long PCR product. Low quality sequences were
389 filtered and trimmed using SICKLE (73) and adapter were removed by using CUTADAPT (74).
390 Subsequent processing of reads were performed by USEARCH and clustered at 60% identity cutoff
391 using cd-hit-est (75). HMMER (76) search was used for taxonomical annotation with manually curated
392 database of *Proteobacteria* and sequences of Podar *et al.* (2015). More details can be found in Bravo *et*
393 *al.* (2018).

394 **Phylogenetic analysis:** A phylogenetic analysis was performed for *hgcA* sequences representative
395 for the OTUs observed for the 34 hotspots and existing *hgcA* entries in our curated database. The
396 sequences were adequately curated and taxonomy homogenized using taxtastic
397 [https://github.com/fhcrc/taxtastic] and the R-package taxize (77). The obtained protein sequences were
398 aligned with MUSCLE (78) (version 3.8.1551). The alignment was trimmed to the size of the amplicon,
399 and a tree was generated using RAxML (79) (version 8.2.4) - with the PROTGAMMLG model and

bioRxiv preprint doi: https://doi.org/10.1101/299248; this version posted April 11, 2018. The copyright holder for this preprint (which was not certified by peer review) is the author/funder, who has granted bioRxiv a license to display the preprint in perpetuity. It is made available under aCC-BY-NC-ND 4.0 International license.

400 autoMR to choose the number of necessary bootstrap resamplings (n = 750). This tree and the
401 corresponding alignment were used to generate a reference package for PPLACER (80). The guppy tool
402 of PPLACER was then used to classify the sequences with a likelihood threshold of 0.8.

403 Statistical analysis

404 Family-level microbial community composition in the different samples were compared using non-
405 metric multidimensional scaling (nMDS) based on Bray-Curtis similarities and using the software
406 PRIMER 7 (81). Information on the common set of samples from community composition based on
407 Bray-Curtis similarities and that from geochemical variables based on Euclidean distance was presented
408 in one single ordination. A combined nMDS plot with bubble and vector plots of geochemical factors
409 projected on the same ordination of community composition was constructed to reveal the relationships
410 between community compositions and potentially explanatory geochemical variables (81). Pearson's
411 correlation coefficient (R) was assessed to reveal linear relationships between variables using a
412 significance level of alpha < 0.05.

413 Acknowledgements

414 This project was carried out within the Swedish-Sino SMaREF (2013-6978) funded by the Swedish
415 Research Council. This study was also supported by the Swedish Energy Agency (grant number 36155-
416 1) and the Swedish Research Council (Grants 2011–7192 and 2012-3892) and Generalitat de Catalunya
417 (Beatriu de Pinos BP-00385-2016). Sequencing was carried out at the SciLifeLab SNP/SEQ facility
418 hosted by Uppsala University and we also acknowledge the Uppsala Multidisciplinary Centre for
419 Advanced Computational Science (UPPMAX) for access to storage and computational resources.

420 References

421 1. UNEP. 2013. Global Mercury Assessment 2013: Sources, Emissions, Releases, and
422 Environmental Transport. UNEP 42.
423 2. Amos HM, Jacob DJ, Streets DG, Sunderland EM. 2013. Legacy impacts of all-time
424 anthropogenic emissions on the global mercury cycle. Global Biogeochem Cycles 27:410–421.
425 3. Lamborg C, Bowman K, Hammerschmidt C, Gilmour C, Munson K, Selin N, Tseng C-M. 2014.
426 Mercury in the Anthropocene Ocean. Oceanography 27:76–87.
427 4. Gu B, Bian Y, Miller CL, Dong W, Jiang X, Liang L. 2011. Mercury reduction and complexation

bioRxiv preprint doi: https://doi.org/10.1101/299248; this version posted April 11, 2018. The copyright holder for this preprint (which was not certified by peer review) is the author/funder, who has granted bioRxiv a license to display the preprint in perpetuity. It is made available under aCC-BY-NC-ND 4.0 International license.

428 by natural organic matter in anoxic environments. Proc Natl Acad Sci 108:1479–1483.

429 5. Drott A, Lambertsson L, Björn E, Skyllberg U. 2007. Importance of dissolved neutral mercury
430 sulfides for methyl mercury production in contaminated sediments. Environ Sci Technol
431 41:2270–2276.

432 6. Johansson K, Tyler G. 2001. Impact of atmospheric long range transport of lead, mercury and
433 cadmium on the Swedish forest environment. Water, Air Soil Pollut Focus 1:279–297.

434 7. Xu J, Bravo AG, Lagerkvist A, Bertilsson S, Sjöblom R, Kumpiene J. 2014. Sources and
435 remediation techniques for mercury contaminated soil. Environ Int 74:42–53.

436 8. Grigal DF. 2002. Inputs and outputs of mercury from terrestrial watersheds: a review. Environ
437 Rev 10:1–39.

438 9. Bravo AG, Bouchet S, Tolu J, Björn E, Mateos-Rivera A, Bertilsson S. 2017. Molecular
439 composition of organic matter controls methylmercury formation in boreal lakes. Nat Commun
440 8:14255.

441 10. Isidorova A, Bravo AG, Riise G, Bouchet S, Björn E, Sobek S. 2016. The effect of lake browning
442 and respiration mode on the burial and fate of carbon and mercury in the sediment of two boreal
443 lakes. J Geophys Res Biogeosciences 121:233–245.

444 11. Hongve D, Haaland S, Riise G, Blakar I, Norton S. 2012. Decline of acid rain enhances mercury
445 concentrations in fish. Environ Sci Technol 46:2490–1.

446 12. Åkerblom S, Nilsson M, Yu J, Ranneby B, Johansson K. 2012. Temporal change estimation of
447 mercury concentrations in northern pike (Esox lucius L.) in Swedish lakes. Chemosphere 86:439–
448 445.

449 13. Gandhi N, Tang RWK, Bhavsar SP, Arhonditsis GB. 2014. Fish mercury levels appear to be
450 increasing lately: A report from 40 years of monitoring in the province of Ontario, Canada.
451 Environ Sci Technol 48:5404–5414.

452 14. Eklöf K, Bishop K, Bertilsson S, Björn E, Buck M, Skyllberg U, Osman OA, Kronberg RM,
453 Bravo AG. 2018. Formation of mercury methylation hotspots as a consequence of forestry
454 operations. Sci Total Environ 613–614:1069–1078.

455 15. Parks JM, Johs A, Podar M, Bridou R, Hurt RA, Smith SD, Tomanicek SJ, Qian Y, Brown SD,
456 Brandt CC, Palumbo A V, Smith JC, Wall JD, Elias DA, Liang L. 2013. The genetic basis for
457 bacterial mercury methylation. Science (80-) 339:1332–1335.

458 16. Tjerngren, Karlsson T, Björn E, Skyllberg U. 2012. Potential Hg methylation and MeHg
459 demethylation rates related to the nutrient status of different boreal wetlands. Biogeochemistry
460 108:335–350.

461 17. Eckley CS, Hintelmann H. 2006. Determination of mercury methylation potentials in the water
462 column of lakes across Canada. Sci Total Environ 368:111–125.

463 18. Monperrus M, Tessier E, Amouroux D, Leynaert A. 2007. Mercury methylation , demethylation
464 and reduction rates in coastal and marine surface waters of the Mediterranean Sea. Mar Chem
465 107:49–63.

466 19. Gascón Díez E, Loizeau J-L, Cosio C, Bouchet S, Adatte T, Amouroux D, Bravo AG. 2016. Role
467 of Settling Particles on Mercury Methylation in the Oxic Water Column of Freshwater Systems.
468 Environ Sci Technol 50:11672–11679.

469 20. Compeau GC, Bartha R. 1985. Sulfate-reducing Bacteria: principal methylators of mercury in
470 anoxic estuarine sediment. Appl Environ Microbiol 50:498–502.

471 21. King JK, Kostka JE, Frischer ME, Saunders FM, Jahnke RA. 2001. A quantitative relationship
472 that demonstrates mercury methylation rates in marine sediments are based on the community
473 composition and activity of sulfate-reducing bacteria. Environ Sci Technol 35:2491–2496.

bioRxiv preprint doi: https://doi.org/10.1101/299248; this version posted April 11, 2018. The copyright holder for this preprint (which was not certified by peer review) is the author/funder, who has granted bioRxiv a license to display the preprint in perpetuity. It is made available under aCC-BY-NC-ND 4.0 International license.

474 22. Fleming EJ, Mack EE, Green PG, Nelson DC. 2006. Mercury methylation from unexpected
475 sources: molybdate-inhibited freshwater sediments and an iron-reducing bacterium. Appl Environ
476 Microbiol 72:457–464.

477 23. Kerin EJ, Gilmour CC, Roden E, Suzuki MT, Coates JD, Mason RP. 2006. Mercury methylation
478 by dissimilatory iron-reducing bacteria. Appl Environ Microbiol 72:7919–7921.

479 24. Hamelin S, Amyot M, Barkay T, Wang Y, Planas D. 2011. Methanogens: principal methylators
480 of mercury in lake periphyton. Environ Sci Technol 45:7693–7700.

481 25. Gilmour CC, Podar M, Bullock AL, Graham AM, Brown SD, Somenahally AC, Johs A, Hurt
482 RA, Bailey KL, Elias DA. 2013. Mercury methylation by novel microorganisms from new
483 environments. Environ Sci Technol 47:11810–11820.

484 26. Jonsson S, Skyllberg U, Nilsson MB, Lundberg E, Andersson A, Björn E. 2014. Differentiated
485 availability of geochemical mercury pools controls methylmercury levels in estuarine sediment
486 and biota. Nat Commun 5:4624.

487 27. Ullrich SM, Tanton TW, Abdrashitova SA, Svetlana A. 2001. Mercury in the aquatic
488 environment : a review of factors affecting methylation. Crit Rev Environ Sci Technol 31:241–
489 293.

490 28. Bigham GN, Murray KJ, Masue-Slowey Y, Henry EA. 2017. Biogeochemical controls on
491 methylmercury in soils and sediments: Implications for site management. Integr Environ Assess
492 Manag 13:249–263.

493 29. Liem-Nguyen V, Skyllberg U, Björn E. 2017. Thermodynamic Modeling of the Solubility and
494 Chemical Speciation of Mercury and Methylmercury Driven by Organic Thiols and Micromolar
495 Sulfide Concentrations in Boreal Wetland Soils. Environ Sci Technol 51:3678–3686.

496 30. Chiasson-Gould SA, Blais JM, Poulain AJ. 2014. Dissolved organic matter kinetically controls
497 mercury bioavailability to bacteria. Environ Sci Technol 48:3153–3161.

498 31. Schaefer JK, Morel FMM. 2009. High methylation rates of mercury bound to cysteine by
499 Geobacter sulfurreducens. Nat Geosci 2:123–126.

500 32. Graham AM, Aiken GR, Gilmour CC. 2013. Effect of dissolved organic matter source and
501 character on microbial Hg methylation in Hg-S-DOM solutions. Environ Sci Technol 47:5746–
502 5754.

503 33. Gilmour CC, Ghosh U, Santillan EFU, Soren A, Bell JT, Butera D, McBurney AW, Brown S,
504 Henry E, and Vlassopoulos D. 2015. Impacts of Activated Carbon Amendment on Hg
505 Methylation, Demethylation and Microbial Activity in Marsh SoilsAGU Fall Meeting.

506 34. Schaefer JK, Kronberg R-M, Morel FMM, Skyllberg U. 2014. Detection of a key Hg methylation
507 gene, hgcA , in wetland soils. Environ Microbiol Rep n/a-n/a.

508 35. Bravo AG, Loizeau JL, Dranguet P, Makri S, Björn E, Ungureanu VG, Slaveykova VI, Cosio C.
509 2016. Persistent Hg contamination and occurrence of Hg-methylating transcript (*hgcA*)
510 downstream of a chlor-alkali plant in the Olt River (Romania). Environ Sci Pollut Res 1–13.

511 36. Bravo AG, Zopfi J, Buck M, Xu J, Bertilsson S, Schaefer JK, Poté J, and Cosio C. 2018.
512 Geobacteraceae are important members of mercury-methylating microbial communities of
513 sediments impacted by wastewater releases. ISME J.

514 37. Liu Y-R, Yu R-Q, Zheng Y-M, He J-Z. 2014. Analysis of the microbial community structure by
515 monitoring an Hg methylation gene (hgcA) in paddy soils along an Hg gradient. Appl Environ
516 Microbiol 80:2874–9.

517 38. Bae HS, Dierberg FE, Ogram A. 2014. Syntrophs dominate sequences associated with the
518 mercury methylation-related gene *hgcA* in the water conservation areas of the Florida Everglades.
519 Appl Environ Microbiol 80:6517–6526.

520 39. Podar M, Gilmour CC, Brandt CC, Soren A, Brown SD, Crable BR, Palumbo A V., Somenahally

bioRxiv preprint doi: https://doi.org/10.1101/299248; this version posted April 11, 2018. The copyright holder for this preprint (which was not certified by peer review) is the author/funder, who has granted bioRxiv a license to display the preprint in perpetuity. It is made available under aCC-BY-NC-ND 4.0 International license.

521 AC, Elias DA. 2015. Global prevalence and distribution of genes and microorganisms involved in
522 mercury methylation. Sci Adv 1:e1500675–e1500675.

523 40. Skyllberg ULF, Qian JIN, Frech W, Xia K. 2002. Distribution of mercury , methyl mercury and
524 organic sulphur species in soil , soil solution and stream of a boreal forest catchment 1:53–76.

525 41. Kronberg RM, Jiskra M, Wiederhold JG, Björn E, Skyllberg U. 2016. Methyl mercury formation
526 in hillslope soils of boreal forests: The role of forest harvest and anaerobic microbes. Environ Sci
527 Technol 50:9177–9186.

528 42. Tjerngren I, Meili M, Björn E, Skyllberg U. 2012. Eight boreal wetlands as sources and sinks for
529 methyl mercury in relation to soil acidity, C/N ratio, and small-scale flooding. Environ Sci
530 Technol 46:8052–8060.

531 43. Yu RQ, Flanders JR, MacK EE, Turner R, Mirza MB, Barkay T. 2012. Contribution of coexisting
532 sulfate and iron reducing bacteria to methylmercury production in freshwater river sediments.
533 Environ Sci Technol 46:2684–2691.

534 44. Ranchou-Peyruse M, Monperrus M, Bridou R, Duran R, Amouroux D, Salvado JC, Guyoneaud
535 R. 2009. Overview of mercury methylation capacities among anaerobic bacteria including
536 representatives of the sulphate-reducers: implications for environmental studies. Geomicrobiol J
537 26:1–8.

538 45. Achá D, Hintelmann H, Pabón CA. 2012. Sulfate-reducing bacteria and mercury methylation in
539 the water column of the Lake 658 of the Experimental Lake Area. Geomicrobiol J 29:667–674.

540 46. King JK, Kostka JE, Frischer ME, Saunders FM. 2000. Sulfate-reducing bacteria methylate
541 mercury at variable rates in pure culture and in marine sediments. Appl Environ Microbiol
542 66:2430–2437.

543 47. Yu RQ, Adatto I, Montesdeoca MR, Driscoll CT, Hines ME, Barkay T. 2010. Mercury
544 methylation in Sphagnum moss mats and its association with sulfate-reducing bacteria in an
545 acidic Adirondack forest lake wetland. FEMS Microbiol Ecol 74:655–668.

546 48. Gilmour CC, Henry EA, Mitchell R. 1992. Sulfate stimulation of mercury methylation in
547 freshwater sediments. Environ Sci Technol 26:2281–2287.

548 49. Plugge CM, Zhang W, Scholten JCM, Stams AJM. 2011. Metabolic flexibility of sulfate-
549 reducing bacteria. Front Microbiol 2.

550 50. McInerney MJ, Struchtemeyer CG, Sieber J, Mouttaki H, Stams AJM, Schink B, Rohlin L,
551 Gunsalus RP. 2008. Physiology, ecology, phylogeny, and genomics of microorganisms capable
552 of syntrophic metabolism. Ann N Y Acad Sci 1125:58–72.

553 51. Pester M, Bittner N, Deevong P, Wagner M, Loy A. 2010. A “rare biosphere” microorganism
554 contributes to sulfate reduction in a peatland. ISME J 4:1–12.

555 52. Wood JM. 1975. Biological cycles for elements in the environment. Naturwissenschaften
556 62:357–364.

557 53. Liu YR, Wang JJ, Zheng YM, Zhang LM, He JZ. 2014. Patterns of Bacterial Diversity Along a
558 Long-Term Mercury-Contaminated Gradient in the Paddy Soils. Microb Ecol 68:575–583.

559 54. Christensen GA, Wymore AM, King AJ, Podar M, Hurt RA, Santillan EU, Soren A, Brandt CC,
560 Brown SD, Palumbo A V., Wall JD, Gilmour CC, Elias DA. 2016. Development and validation
561 of broad-range aualitative and clade-specific quantitative molecular probes for assessing mercury
562 methylation in the environment. Appl Environ Microbiol 82:6068–6078.

563 55. Skyllberg U, Drott A, Lambertsson L, Bjorn E, Karlsson T, Johnson T, Heinemo SA, Holmstrm
564 H. 2007. Net methylmercury production as a basis for improved risk assessment of mercury-
565 contaminated sediments. Ambio 36:437–442.

566 56. Drott A, Lambertsson L, Björn E, Skyllberg U. 2008. Do potential methylation rates reflect
567 accumulated methyl mercury in contaminated sediments? Environ Sci Technol 42:153–158.

bioRxiv preprint doi: https://doi.org/10.1101/299248; this version posted April 11, 2018. The copyright holder for this preprint (which was not certified by peer review) is the author/funder, who has granted bioRxiv a license to display the preprint in perpetuity. It is made available under aCC-BY-NC-ND 4.0 International license.

568 57. Remy S, Prudent P, Probst JL. 2006. Mercury speciation in soils of the industrialised Thur River
569 catchment (Alsace, France). Appl Geochemistry 21:1855–1867.

570 58. Hunger S, Gößner AS, Drake HL. 2015. Anaerobic trophic interactions of contrasting methane-
571 emitting mire soils: Processes versus taxa. FEMS Microbiol Ecol 91:1–14.

572 59. Ransom-Jones E, Jones DL, McCarthy AJ, McDonald JE. 2012. The Fibrobacteres: An Important
573 Phylum of Cellulose-Degrading Bacteria. Microb Ecol 63:267–281.

574 60. Podosokorskaya OA, Kadnikov V V., Gavrilov SN, Mardanov A V., Merkel AY, Karnachuk O
575 V., Ravin N V., Bonch-Osmolovskaya EA, Kublanov I V. 2013. Characterization of
576 Melioribacter roseus gen. nov., sp. nov., a novel facultatively anaerobic thermophilic cellulolytic
577 bacterium from the class Ignavibacteria, and a proposal of a novel bacterial phylum
578 Ignavibacteriae. Environ Microbiol 15:1759–1771.

579 61. Liang B, Wang LY, Mbadinga SM, Liu JF, Yang SZ, Gu JD, Mu BZ. 2015. Anaerolineaceae and
580 Methanosaeta turned to be the dominant microorganisms in alkanes-dependent methanogenic
581 culture after long-term of incubation. AMB Express 5.

582 62. Juottonen H, Eiler A, Biasi C, Tuittila E-S, Yrjälä K, Fritze H. 2017. Distinct Anaerobic Bacterial
583 Consumers of Cellobiose-Derived Carbon in Boreal Fens with Different CO2 /CH4 Production
584 Ratios. Appl Environ Microbiol 83:e02533-16.

585 63. Kuever J. 2014. The family desulfobulbaceae, p. 75–86. *In* The Prokaryotes: Deltaproteobacteria
586 and Epsilonproteobacteria.

587 64. Holmes DE, Shrestha PM, Walker DJF, Dang Y, Nevin KP, Woodard TL, Lovley DR. 2017.
588 Metatranscriptomic evidence for direct interspecies electron transfer between *Geobacter* and
589 *Methanothrix* species in methanogenic rice paddy soils. Appl Environ Microbiol 2.

590 65. WRB. 2014. World Reference Base for Soil Resources 2014, update 2015. International soil
591 classification system for naming soils and creating legends for soil maps. World Soil Resources
592 Reports No. 106World Soil Resources Reports No. 106.

593 66. Eklöf K, Meili M, Åkerblom S, von Brömssen C, Bishop K. 2013. Impact of stump harvest on
594 run-off concentrations of total mercury and methylmercury. For Ecol Manage 290:83–94.

595 67. Löfgren S, Ring E, von Brömssen C, Sørensen R, Högbom L. 2009. Short-term effects of clear-
596 cutting on the water chemistry of two boreal streams in northern Sweden: a paired catchment
597 study. Ambio 38:347–356.

598 68. Lambertsson L, Lundberg E, Nilsson M, Frech W. 2001. Applications of enriched stable isotope
599 tracers in combination with isotope dilution GC-ICP-MS to study mercury species transformation
600 in sea sediments during in situ. J Anal At Spectrom 16:1296–1301.

601 69. Sinclair L, Osman OA, Bertilsson S, Eiler A. 2015. Microbial community composition and
602 diversity via 16S rRNA gene amplicons: Evaluating the Illumina platform. PLoS One
603 10:e0116955.

604 70. Edgar RC. 2013. UPARSE: highly accurate OTU sequences from microbial amplicon reads. Nat
605 Methods 10:996–8.

606 71. Edgar RC, Flyvbjerg H. 2015. Error filtering, pair assembly and error correction for next-
607 generation sequencing reads. Bioinformatics 31:3476–3482.

608 72. Edgar R. 2016. SINTAX: a simple non-Bayesian taxonomy classifier for 16S and ITS sequences.
609 bioRxiv 74161.

610 73. Joshi NA, Fass JN. 2011. Sickle: A sliding-window, adaptive, quality-based trimming tool for
611 FastQ files.

612 74. Martin M. 2011. Cutadapt removes adapter sequences from high-throughput sequencing reads.
613 EMBnet.journal 17:10–12.

bioRxiv preprint doi: https://doi.org/10.1101/299248; this version posted April 11, 2018. The copyright holder for this preprint (which was not certified by peer review) is the author/funder, who has granted bioRxiv a license to display the preprint in perpetuity. It is made available under aCC-BY-NC-ND 4.0 International license.

614 75. Fu L, Niu B, Zhu Z, Wu S, Li W. 2012. CD-HIT: Accelerated for clustering the next-generation
615 sequencing data. Bioinformatics 28:3150–3152.

616 76. Eddy SR. 2011. Accelerated profile HMM searches. PLoS Comput Biol 7:e1002195.

617 77. Chamberlain SA, Szöcs E. 2013. taxize: taxonomic search and retrieval in R. F1000Research
618 2:191.

619 78. Edgar RC. 2004. MUSCLE: Multiple sequence alignment with high accuracy and high
620 throughput. Nucleic Acids Res 32:1792–1797.

621 79. Stamatakis A. 2014. RAxML version 8: A tool for phylogenetic analysis and post-analysis of
622 large phylogenies. Bioinformatics 30:1312–1313.

623 80. Matsen FA, Kodner RB, Armbrust EV. 2010. pplacer: Linear time maximum-likelihood and
624 Bayesian phylogenetic placement of sequences onto a fixed reference tree. BMC Bioinformatics.

625 81. Clarke KR, Gorley RN. 2015. PRIMER v7: User Manual/Tutorial. Prim Plymouth UK 192 p.

626

bioRxiv preprint doi: https://doi.org/10.1101/299248; this version posted April 11, 2018. The copyright holder for this preprint (which was not certified by peer review) is the author/funder, who has granted bioRxiv a license to display the preprint in perpetuity. It is made available under aCC-BY-NC-ND 4.0 International license.

627 **Table 1.** Comparison of the relative abundances (%) of the most abundant taxa (phylum level) in all the samples
628 (n=200) with the 34 MeHg hotspots based on 16S rRNA sequences. Relative abundances of classes under phylum
629 *Proteobacteria* are listed with indent (SD: Standard deviation)

Most abundant taxa	Mean ± SD		Maximum		Minimum	
	All samples	Hotspots	All samples	Hotspots	All samples	Hotspots
Acidobacteria	36.11 ±10.53	25.57 ±8.77	73.64	49.29	8.10	9.40
Proteobacteria	13.99 ±4.03	16.56 ±2.96	28.13	27.60	2.90	8.87
Alphaproteobacteria	6.83 ±3.01	7.13 ±2.81	16.43	13.95	1.77	2.66
Deltaproteobacteria	3.31 ±1.69	3.56 ±1.38	13.36	7.15	0.71	1.30
Gammaproteobacteria	2.06 ±1.33	1.48 ±0.76	7.15	3.66	0.24	0.35
Betaproteobacteria	1.78 ±2.13	4.14 ±2.47	11.11	10.46	0.00	0.65
Epsilonproteobacteria	0.01 ±0.03	0.03 ±0.06	0.30	0.24	0.00	0.00
Planctomycetes	8.18 ±4.21	5.82 ±2.77	24.82	11.64	1.36	1.95
Bacteroidetes	6.61 ±5.24	11.38 ±7.92	51.60	51.60	0.41	1.60
Parcubacteria	6.35 ±4.19	9.01 ±5.14	26.36	24.47	0.06	2.13
Verrucomicrobia	6.28 ±2.78	5.30 ±2.31	14.89	10.64	0.65	0.65
Thaumarchaeota	3.96 ±2.77	2.53 ±2.44	18.44	14.83	0.00	0.00
Actinobacteria	3.11 ±2.38	2.94 ±1.62	19.86	6.03	0.47	0.89
Chlamydiae	2.83 ±2.56	1.31 ±1.08	22.87	3.71	0.24	0.30
Chloroflexi	2.60 ±3.18	7.16 ±5.18	17.79	15.19	0.00	0.12
Others	9.97 ±0.89	12.41 ±1.66	17.14	8.98	0.00	0.00

630
631

bioRxiv preprint doi: https://doi.org/10.1101/299248; this version posted April 11, 2018. The copyright holder for this preprint (which was not certified by peer review) is the author/funder, who has granted bioRxiv a license to display the preprint in perpetuity. It is made available under aCC-BY-NC-ND 4.0 International license.

632

633 **Table 2.** Moderate (0.5≤R<0.7) to weak (0.3≤R<0.5) Pearson correlations between families and %MeHg in all
634 samples based on 16S rRNA. Families potentially involved in Hg methylation were marked in bold.

Families	Correlations with %MeHg
Unclassified Fibrobacterales	0.56
Methanothrix	0.54
Unclassified Ignavibacteriales	0.52
Spirochaetaceae	0.52
Holophagaceae	0.50
Anaerolineaceae	0.41
Lentimicrobiaceae	0.40
Syntrophobacteraceae	0.39
Unclassified Phycisphaerales	0.37
Methanosarcinaceae	0.37
Methanoregulaceae	0.35
Desulfobulbaceae	0.35
Porphyromonadaceae	0.35
Rhodobiaceae	0.33
Unclassified Clostridiales	0.32
Gemmatimonadaceae	0.30
Syntrophaceae	0.30
Unclassified Omnitrophica	0.30
Nitrosomonadaceae	0.30
Desulfobacteraceae	0.30
Dehalococcoidaceae	0.30
Unclassified Obscuribacterales	-0.30
Unclassified Solibacterales	-0.33
Tepidisphaeraceae	-0.38

635

bioRxiv preprint doi: https://doi.org/10.1101/299248; this version posted April 11, 2018. The copyright holder for this preprint (which was not certified by peer review) is the author/funder, who has granted bioRxiv a license to display the preprint in perpetuity. It is made available under aCC-BY-NC-ND 4.0 International license.

636 **Table 3.** Relative abundance of families involved in $Hg^{(II)}$ methylation based on *hgcA* sequences in 34 hotspots.

Families	**Örebro**	**Balsjö**	**Strömsjöliden**
	% of *hgcA* reads	% of *hgcA* reads	% of *hgcA* reads
Unclassified Deltaproteobacteria	43.24±37.11	44.85±30.09	55.69±18.23
Geobacteraceae	26.79±31.09	24.62±22.22	39.40±18.96
Unclassified Bacteria	10.72±17.45	25.58±33.67	1.43±1.02
Ruminococcaceae	9.12±18.23	1.52±2.30	0.15±0.04
Unclassified	6.62±8.65	2.37±3.86	1.27±2.98
Unclassified Euryarchaeota	0.84±2.22	0.02±0.02	0.01±0.02
Desulfovibrionaceae	0.83±1.28	0.16±0.03	0.02±0.04
Unclassified Methanomicrobiales	0.49±1.21	0.06±0.09	0.03±0.12
Syntrophaceae	0.35±0.45	0.05±0.00	0.00±0.00
Methanomassiliicoccaceae	0.31±0.53	0.02±0.00	0.13±0.05
Methanoregulaceae	0.20±0.03	0.06±0.03	0.00±0.01
Syntrophomonadaceae	0.17±0.13	0.02±0.03	0.13±0.04
Unclassified Desulfovibrionales	0.14±0.15	0.02±0.05	0.03±0.04
Unclassified Clostridiales	0.06±0.22	0.51±0.19	0.08±0.07
Unclassified Firmicutes	0.06±0.02	0.00±0.00	0.00±0.00
Unclassified Desulfuromonadales	0.03±0.00	0.10±0.03	0.39±0.32
Desulfobulbaceae	0.02±0.02	0.01±0.00	0.00±0.01
Desulfuromonadaceae	0.01±0.01	0.00±0.04	0.00±0.04
Syntrophorhabdaceae	0.01±0.00	0.00±0.02	0.00±0.06
Unclassified Deferrisoma	0.01±0.00	0.00±0.00	1.18±0.98
Desulfarculaceae	0.00±0.02	0.00±0.00	0.00±0.02
Pelobacteraceae	0.00±0.01	0.01±0.01	0.07±0.03

637

bioRxiv preprint doi: https://doi.org/10.1101/299248; this version posted April 11, 2018. The copyright holder for this preprint (which was not certified by peer review) is the author/funder, who has granted bioRxiv a license to display the preprint in perpetuity. It is made available under aCC-BY-NC-ND 4.0 International license.

638
639
640 **Figure 1.** Non-metric multidimensional scaling (nMDS) of microbial community composition of all samples
641 (family level based on 16S rRNA) overlaid with families (black lint) and geochemical factors (dotted brown line)
642 moderately correlated with biotic ordination (correlation coefficients > 0.5) (%MeHg: MeHg/THg). Relative
643 dissimilarities (or distances) among the samples were computed according to the resemblance matrix
644 calculated on fourth rooted family reads.
645
646 **Figure 2.** Non-metric multidimensional scaling (nMDS) of potential Hg methylators (family level based on *hgcA*)
647 in 34 hotspots overlaid with geochemical factors that were moderately correlated with the biotic ordination
648 positions (correlation coefficients > 0.5)
649
650 **Figure 3.** Phylogenetic relationships of *Deltaproteobacterial hgcA* sequences in the studied forest soils. The 20
651 most abundant *Deltaproteobacteria* are in blue. The OTUs taxonomically assigned as *Geobacter* are indicated in
652 the plot "*Geobacter sp.*". OTUs non-taxonomically assigned are presented as "OTU". Reference genomes are
653 marked in brown. The tree was generated using RAxML (version 8.2.4) with the PROTGAMMLG model and the
654 autoMR to choose the number of necessary bootstraps (750). Please see details of the collapsed tree in the Fig.
655 S2.
656

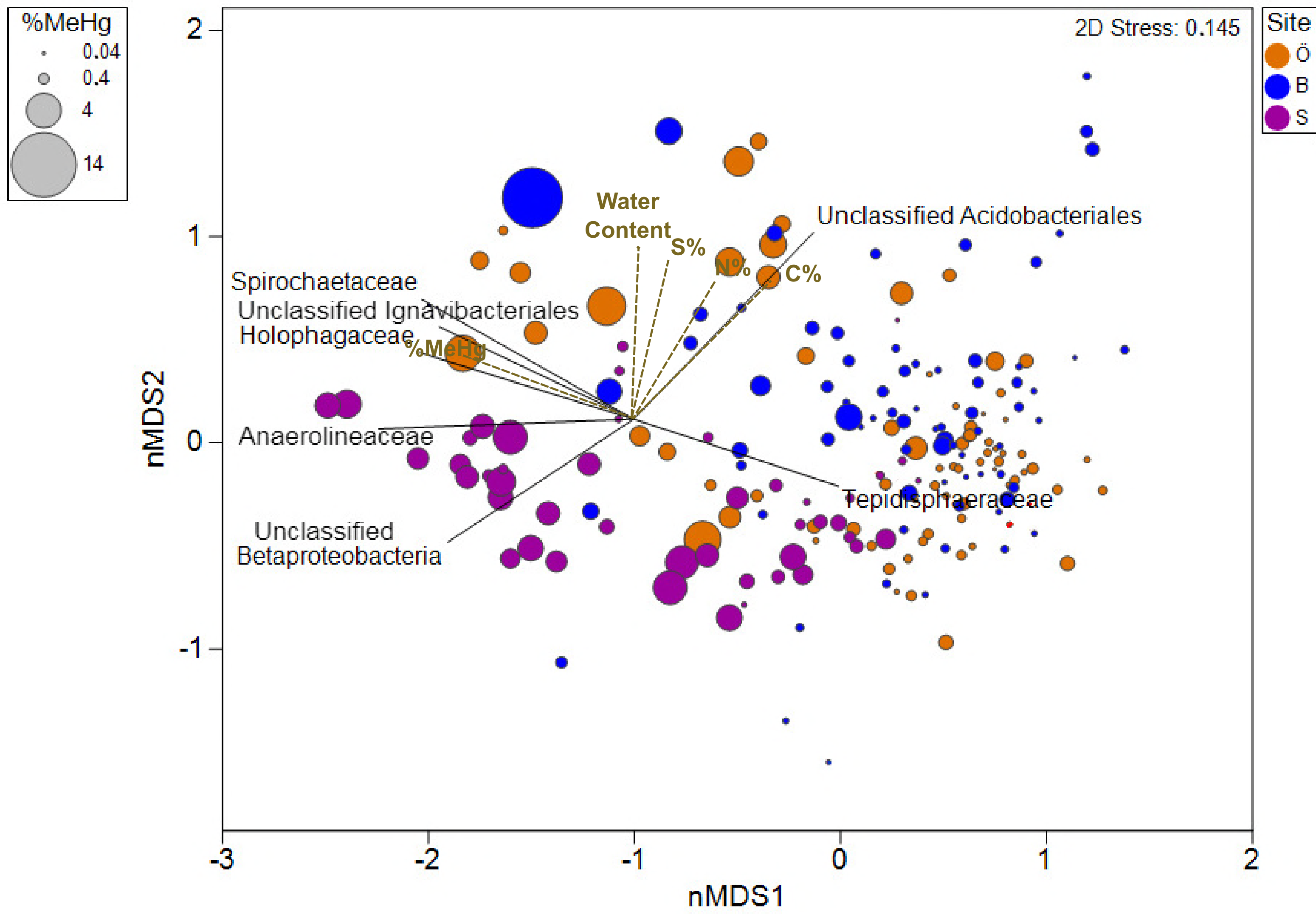
%MeHg
0.04
0.4
4
14
2D Stress: 0.145
Site
Ö
B
S
Water
Content
S%
N%
C%
Unclassified Acidobacteriales
Spirochaetaceae
Unclassified Ignavibacteriales
Holophagaceae
%MeHg
Anaerolineaceae
Tepidisphaeraceae
Unclassified
Betaproteobacteria
nMDS2
nMDS1
2
1
0
-1
-3
-2
-1
0
1
2

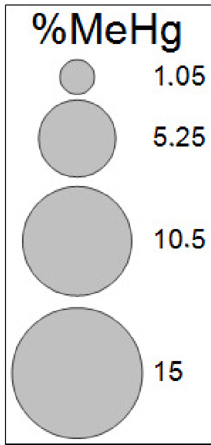

2D Stress: 0.122

Site
Ö
B
S

Geobacteraceae
Unclassified
Desulfuromonadales
Ruminococcaceae
Unclassified
Desulfovibrionaceae
Unclassified Desulfovibrionales
S%
Unclassified Bacteria
C/S
Unclassified
Deltaproteobacteria

1
0
-1
nMDS2

-1
0
1
2
nMDS1

Geobacter_sulfurreducens_PCA_01436
Geobacter_sulfurreducens_AM_1_02229
Geobacter_soli_GSS01_01622
OTU_0042
Geobacter sp.
OTU_0057 (2.1%)
OTU_0041 (1%)
OTU_0036
OTU_0249 (1.8%)
OTU_0050
OTU_0075
Geobacter sp.
Geobacter sp (6.6%)
OTU_0085
Geobacter_uraniireducens_Rf4_00504
Geobacter_argillaceus_ATCC_BAA_1139_02637
OTU_0119
Geobacter_pickeringii_G13__complete_genome__00972
OTU_0626
OTU_0046 (1%)
Geobacter sp.
OTU_0158
OTU_0059
OTU_0101
OTU_0073
OTU_0056 (1%)
OTU_0283
OTU_0031
OTU_0244
OTU_0014
OTU_0180
Geobacter_metallireducens_GS15
Pelobacter_seleniigenes_DSM_18267_01952
Syntrophus_sp._G20_Ga0063310_01376
OTU_0188
OTU_0122
OTU_0185
OTU_0108
OTU_0044 (1.2%)
OTU_0013 (2.4%)
OTU_0218
OTU_0012 (4.4%)
OTU_0071
OTU_0147
Geobacter sp.
Geobacter sp.
Geobacter sp.
OTU_0005 (14.2%)
OTU_0215
Geobacter sp.
Geobacter sp.
OTU_0266
Geobacter sp.
Geobacter sp.
Geobacter sp.
Geobacter sp.
Geobacter sp.
Geobacter sp. (3.1%)
OTU_0674
OTU_0019
Geobacter sp.
Geobacter sp.
Geobacter sp.
Geobacter sp.
Geobacter sp.
Geobacter sp.
Geobacter_sp._OR_1_02594
OTU_0060 (2.7%)
OTU_0051 (2.2%)
Geobacter sp. (1.4%)
OTU_0308
Geobacter sp. (2.3%)
Geobacter sp.
OTU_0705 (8.3%)
Geobacter sp.
Geobacter sp.
Geobacter sp.
Geobacter_sp._FRC_32_02506
Geobacter_sp_FRC32
Geobacter sp.
Geobacter sp. (2%)
Geobacter sp.
Geobacter sp. (3.3%)
Geobacter sp.
Geobacter sp. (2.1%)
Geobacter sp.
Geobacter sp.
Geobacter_bremensis_R1_03513
Geobacter sp. (2.2%)
Geobacter sp.
Geobacter sp.
Geobacter sp.
Geobacter_sp._M18_01045
Geobacter sp.
OTU_0202
OTU_0373
Geobacter sp.

84 OTUs
Geobacter sp. FRC32
Geobacter sulfurreducens PCA
Geobacter metallireducens GS15
Pelobacter seleniigenes DSM
Geobacter tremensis R1 03513
3 OTUs
Methanospirillum hungatei JF1
Methanomassiliicoccus luminyensis B10
1 OTUs
Syntrophus aciditrophicus
delta proteobacterium NaphS2
Syntrophorhabdus aromaticivorans UI
4 OTUs
Ethanoligenens harbinenseYUAN3
Dehalobacter sp CF
Clostridium_termitidis_CT1112
4 OTUs
Desulfovibrio desulfuricans ND132
Desulfobulbus propionicus DSM 2032
Desulfomicrobium baculatum
Deferrisoma camini S3R1
8 OTUs
Dethiobacter alkaliphilus AHT_1
Desulfomonile tiedjei DCB1 DSM 6799